

Proposed theory to determine the horizontal shear between composite precast and in situ concrete

Mitchell Gohnert *

Department of Civil Engineering, University of the Witwatersrand, Private Bag 3, P.O. Wits, 2050, Johannesburg, South Africa

Received 7 June 2000; accepted 25 August 2000

Abstract

A theory is proposed to determine the horizontal shear between the roughened interface of a composite precast member and in situ concrete. The proposed method is completely congruous with the alternative method listed in clause 17.5.3 of ACI 318-95. The horizontal shear is determined by calculating the change in the tension force across an elemental segment at the point maximum shear will occur. This approach differs from prevailing methods which base the horizontal shear as a function of the mid-span ultimate force. Equations are developed for both cracked and uncracked sections. Experiments were also performed to validate the proposed equations. © 2000 Elsevier Science Ltd. All rights reserved.

Keywords: Reinforced concrete; Precast concrete; Shear; Horizontal shear; Design; Composites

1. Introduction

In ACI 318-95 [1], several methods are given to determine the horizontal shear. The foremost is a method based on the vertical shear (Section 17.5.2). Additional methods referred to as the shear friction method (Section 11.7) and the alternative method (Section 17.5.3) are also given. Although this later method is referred to as the “alternative method”, it is the only method prescribed by many other international codes such as BS 8110 [2] and SABS 0100 [3]. As stated by ACI 318-95,

17.5.3 – As an alternative to 17.5.2, horizontal shear shall be determined by computing the actual change in compressive or tensile force in any segment, and provisions shall be made to transfer that force as horizontal shear to the supporting element. The factored shear force shall not exceed horizontal shear strength ϕV_{nh} as given in Sections 17.5.2.1 through 17.5.2.4, where area of contact surface A_c shall be substituted for $b_v d$.

In the past, many designers assumed that the shear transferred is an average force over the length of the

contact area; no attempt was made to distribute this force in accordance with the shape of the shear diagram. Since earlier versions of ACI 318 did not give any guidance in this respect, the design procedures followed composite concrete/steel design techniques [4,5]. The slip between composite concrete and steel is relatively large due to the differences in stiffness of each material. This causes a redistribution of force along the length of the contact surface and therefore an average stress can be assumed. In the latest version of ACI 318, a commentary note was included stating that in composite construction, where both materials are concrete, the slip is small and therefore the redistribution of stress is limited and confined to a small region. For this reason, the average stress must be distributed according to the shape of the shear diagram.

R17.5.3.1 – The distribution of horizontal shear stresses along the contact surface in a composite member will reflect the distribution of shear along the member.

In a simply supported beam loaded by a uniformly distributed load, the maximum shear stress at the support is double the average stress. The inclusion of the commentary note, on how the shear should be distributed, has serious ramifications on the design of

* Tel.: +27-11-716-2459; fax: +27-11-339-1762.

E-mail address: gohnert@civen.civil.wits.ac.za (M. Gohnert).

composite members. In many cases, the horizontal shear is now the “bottle neck” of the design since the design must now account for a much higher shear stress. In response, a new theoretical approach is proposed to assess the horizontal shear.

In many international codes, such as those previously cited, the horizontal shear is determined as the mid-span force calculated from the ultimate bending moment. Usually, this mid-span force is the ultimate strength of the reinforcing or prestressing steel. This is clearly a conservative approach. The shear force cannot exceed this value since the member, at ultimate load, is subjected to impending flexural failure. In the past, several theories have been recommended to determine the horizontal shear [6–11]. However, the proposed method differs in a sense that the horizontal shear is determined by calculating the change in the tension stress across a differential segment at the point at which the shear is to be determined. This gives a better representation of the actual shear and remains congruent with Section 17.5.3 of ACI 318-95 [4].

Prior to developing the proposed horizontal shear theory, fundamentals of the ACI’s alternative theory are given (the proposed theory is an extension of the alternative theory). Experiments were also performed to validate the proposed equations.

2. Fundamentals of the alternative theory (Section 17.5.3 of ACI 318)

Bending and shear forces applied to a section of beam are illustrated in Fig. 1. By summing forces about point *a*, a fundamental relationship between the vertical shear (*V*) and the bending moment (*M*) is derived.

$$V = \frac{dM}{dx}. \quad (1)$$

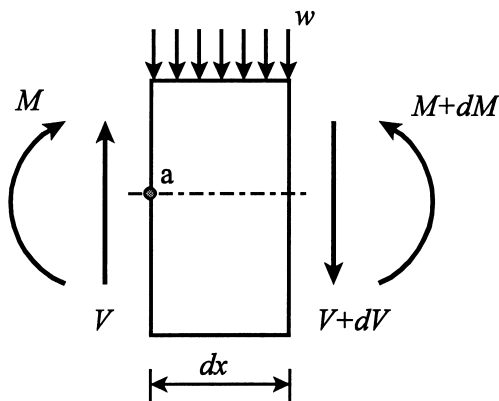


Fig. 1. Differential segment of a beam.

As indicated by Eq. (1), the shear is directly related to the bending moment. Shear will only exist if there is a change in the moment. It is common to separate the two forces and analyse each separately. But in reality, shear is dependant on the bending moment and should be viewed jointly.

The bending moment will cause a stress distribution as depicted in Fig. 2(a). If we cut along the line *b–c* of the segment, the horizontal shear force along that surface is the difference between the resultant forces (see Fig. 2(b)).

$$\sum F = -V_h - F + (F + dF) = 0, \quad (2)$$

$$V_h = (F + dF) - F, \quad (3)$$

where V_h is the horizontal shear force and *F* is the resultant force of the stress distribution.

The stress is simply the shear force divided by the contact interface of the segment.

$$v_h = \frac{(F + dF) - F}{dx} \frac{1}{b_v} = \frac{dF}{dx} \frac{1}{b_v}. \quad (4)$$

The length of the differential segment in Fig. 2 is *dx*. If we consider a much larger segment equal to half the span length (i.e., from the support to mid-span – see Fig. 3) our definition of the horizontal shear is simplified. In a simply supported beam, subjected to a uniformly distributed load, the bending stress at the support is zero and therefore the resultant force (*F*) is zero. Summing forces in Fig. 3,

$$\sum F = V_h = F + dF, \quad (5)$$

where the resultant force (*F + dF*) at mid-span is the ultimate strength of the reinforcement or prestressing steel.

$$V_h = \phi f_y A_s, \quad (6)$$

where ϕ is the strength or material factor, f_y is the yield strength of the steel and A_s is the area of the steel.

The average shear stress over the length *l/2* is then determined by dividing the shear force by the area of the contact interface.

$$v_{h(ave)} = \frac{2V_h}{lb_v}, \quad (7)$$

where $v_{h(ave)}$ is the average horizontal shear stress, *l* the span length and b_v is the width of the contact interface.

Distributing this force according to the shape of the vertical shear diagram, the horizontal shear stress can be determined at any point (*x*) along the length of the span.

$$v_h = \frac{V_h}{b_v} \left(\frac{-8x}{l^2} + \frac{4}{l} \right) \quad (0 \leq x \leq l/2). \quad (8)$$

In a simply supported beam loaded by a uniformly distributed load, the maximum shear stress $v_{h(max)}$ will

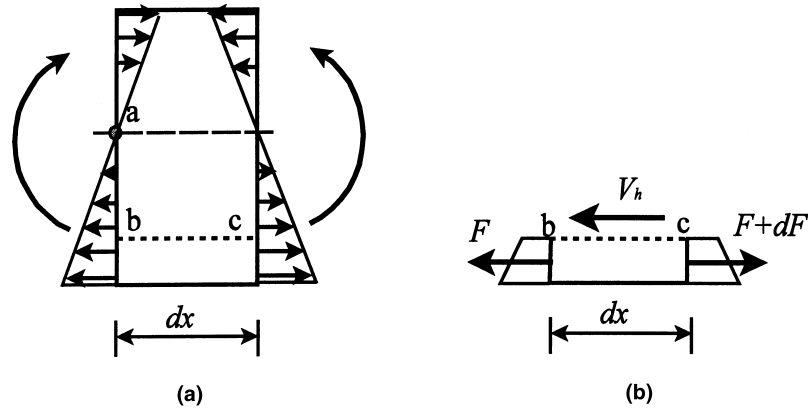


Fig. 2. (a) Bending stress distribution in a segment. (b) Resultant forces and the horizontal shear force along the cut surface $b-c$.

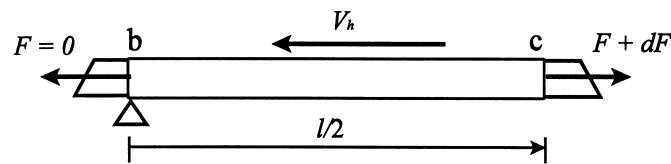


Fig. 3. Horizontal shear force and resultant forces in a beam segment of length $l/2$.

occur at the support. We therefore take the limit of Eq. (8) as $x \rightarrow 0$.

$$v_{h(\max)} = \lim_{x \rightarrow 0} \frac{V_h}{b_v} \left(\frac{-8x}{l^2} + \frac{4}{l} \right) = \frac{4V_h}{lb_v}. \quad (9)$$

The above procedure is the prevailing method used by many international codes. The theory is conservative and safe, but a refinement is possible. As the shear increases towards the supports, the resultant force conversely decreases due to a reducing moment. This decrease in the resultant force can be accounted for and will therefore reduce the horizontal shear stress.

3. Proposed theory to determine the horizontal stress

The equations derived here are applicable to a simply supported beam, loaded by a uniformly distributed load. In addition, the precast member and the contact interface are assumed to be located in the tension zone. Fig. 4 illustrates the assumed configuration. For all other

cases, the equations are easily modified. Since the concrete may or may not be cracked at the location of critical shear, equations will be developed for both cases.

3.1. Horizontal shear stress of an uncracked section

In the composite member, three material properties will be present: the in situ concrete, the precast concrete and the reinforcing or prestressing steel. An analysis would require that at least two materials are transformed into the third. To do so, two modular ratios are defined:

$$\eta_{cc} = \frac{E_{rib}}{E_{in \text{ situ}}}, \quad (10)$$

$$\eta_{cs} = \frac{E_{steel}}{E_{in \text{ situ}}}. \quad (11)$$

The precast member and the steel are transformed into the same material as the in situ concrete. The transformed section is illustrated in Fig. 5. The gross moment of inertia (I_g) is based on this transformed section.

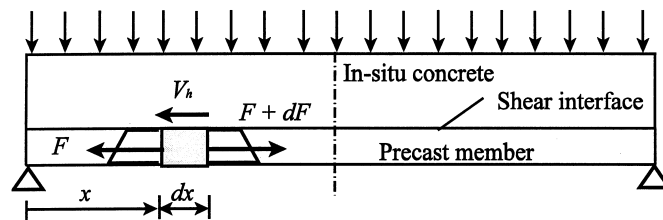


Fig. 4. Composite member and differential element.

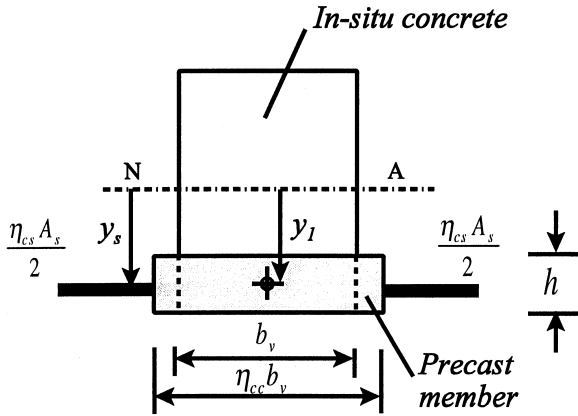


Fig. 5. Transformed uncracked section.

Since the section is assumed to be uncracked, the resultant force in the precast member is composed of two parts – the stress in the concrete and the stress in the steel.

$$f_c = \frac{\eta_{cc} M y_1}{I_g}, \quad (12)$$

$$f_s = \frac{\eta_{cs} M y_s}{I_g}. \quad (13)$$

The term f_c is the average stress in the precast member, f_s is the stress in the steel, y_1 is the distance from the neutral axis to the centre of the precast member and y_s is the distance from the neutral axis to the steel centroid.

The resultant force of each material is simply the stress multiplied by the cross-sectional area of each material. The total force is the sum of the two.

$$F = \frac{\eta_{cc} M y_1 b_v h}{I_g} + \frac{\eta_{cs} M y_s A_s}{I_g} \quad (14)$$

or

$$F = \frac{M \Omega}{I_g}, \quad (15)$$

where $\Omega = \eta_{cc} y_1 b_v h + \eta_{cs} y_s A_s$.

The bending moment for a simply supported beam, loaded by a uniformly distributed load (w), is given in Eq. (16).

$$M = \frac{w l x}{2} \left(1 - \frac{x}{l} \right). \quad (16)$$

Eq. (16) is substituted into Eq. (15) to solve for the resultant forces on either side of the differential element (see Fig. 4) in terms of the bending moment.

$$F = \frac{w l x}{2 I_g} (1 - x/l) \Omega, \quad (17)$$

$$F + dF = \frac{w l (x + dx)}{2 I_g} [1 - (x + dx)/l] \Omega. \quad (18)$$

Substituting Eqs. (17) and (18) into Eq. (4), the horizontal shear stress is defined at any point along the length of the beam.

$$v_h = \frac{w l \Omega}{2 I_g b_v} \frac{(x + dx)[1 - (x + dx)/l] - x(1 - x/l)}{dx} \quad (0 \leq x \leq l/2). \quad (19)$$

In a simply supported beam, subjected to a uniformly distributed load, the maximum shear will occur at the support. We therefore take the limit of Eq. (19) as $x \rightarrow 0$. The resulting equation is simplified by eliminating higher order terms.

$$v_{h(\max)} = \lim_{x \rightarrow 0} \frac{w l \Omega}{2 I_g b_v} \frac{(x + dx)[1 - (x + dx)/l] - x(1 - x/l)}{dx} = \frac{w l \Omega}{2 I_g b_v}. \quad (20)$$

Expressing Eq. (19) in expanded form,

$$v_{h(\max)} = \frac{w l}{2 I_g b_v} [\eta_{cc} y_1 b_v h + \eta_{cs} y_s A_s]. \quad (21)$$

3.2. Horizontal shear stress of a cracked section

The derivation for the cracked case is similar to the uncracked case. The first step is to solve for the transformed cracked section (see Fig. 6).

For the cracked case, the tension stress is assumed to be resisted solely by the reinforcement or pretensioned steel. The stress in the steel is determined by Eq. (22).

$$f_s = \frac{\eta_{cs} M y_s}{I_{cr}}. \quad (22)$$

The resultant force is equal to the stress multiplied by the area of steel.

$$F = \frac{\eta_{cs} M y_s A_s}{I_{cr}}. \quad (23)$$

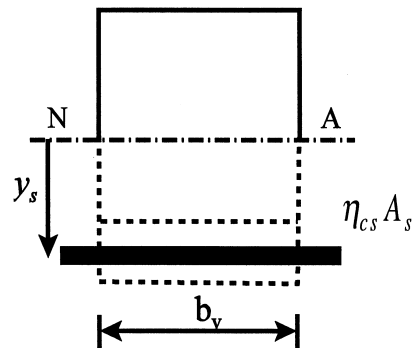


Fig. 6. Transformed cracked section.

Expressed in a simplified form,

$$F = \frac{M\lambda}{I_{cr}}, \quad (24)$$

where $\lambda = \eta_{cs} \nu_s A_s$.

Similar to the uncracked derivation, the bending moment equation (Eq. (16)) is substituted into Eq. (24) to solve for the resultant forces on either side of the differential element (see Fig. 4).

$$F = \frac{wlx(1 - x/l)\lambda}{2I_{cr}}, \quad (25)$$

$$F = \frac{wl(x + dx)[(1 - (x + dx)/l)]\lambda}{2I_{cr}}. \quad (26)$$

Substituting Eqs. (25) and (26) into Eq. (4), the horizontal shear stress is defined at any point along the length of the beam.

$$v_h = \frac{wl\lambda}{2I_{cr}b_v} \frac{(x + dx)[1 - (x + dx)/l] - x(1 - x/l)}{dx} \quad (0 \leq x \leq l/2). \quad (27)$$

In a simply supported beam, subjected to a uniformly distributed load, the maximum shear will occur at the support. We therefore take the limit of Eq. (27) as $x \rightarrow 0$. The resulting equation is simplified by eliminating higher order terms.

$$v_{h(max)} = \lim_{x \rightarrow 0} \frac{wl\lambda}{2I_{cr}b_v} \frac{(x + dx)[1 - (x + dx)/l] - x(1 - x/l)}{dx} = \frac{wl\lambda}{2I_{cr}b_v}. \quad (28)$$

Expressing Eq. (28) in expanded form,

$$v_{h(max)} = \frac{\eta_{cs} w l y_s A_s}{2I_{cr} b_v}. \quad (29)$$

4. Experiments

A total of six composite beams were tested in flexure to determine validity of the above equations. The basic dimension and load arrangement of each of the test beams are given in Fig. 7. A uniformly distributed load is approximated by four point loads as illustrated. The contact width was reduced by 50 mm by wedge-shaped formers placed on either side of the precast member. The precast members are prestressed with 4 mm diameter strands. The prestressing information and concrete strengths are given in Table 1.

Each precast member was lightly brushed on the contact surface and no shear links were provided. The average roughness amplitude of the brushed surface is 0.94 mm (an average of 15 readings). The indentations caused by the brush formed regular rows perpendicular

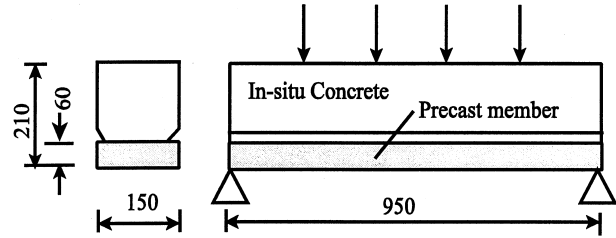


Fig. 7. Basic dimension of the test beams bent in flexure.

to the direction of applied shear. The wavelength ranged from 3 to 4 mm. The actual wavelength was used rather than an assumed value.

In prior tests (not recorded here), the mode of failure was vertical shear in the in situ concrete. The shear crack followed a typical shear pattern – shear cracks extending from the support at an inclination from 30° to 40°. Beams A1 through A6 contained shear reinforcement in the in situ concrete – 4 mm diameter high tensile steel spaced at 100 mm to prevent vertical shear failure. The mode of failure then switched to a horizontal shear failure as illustrated in Fig. 8. This failure was dramatic and seemingly instantaneous. The failure line extends from the support, along the contact surface and then vertical between the shear reinforcement. The length of the failure line along the contact interface did not remain localized as expected [1], but ranged from 50 to 332 mm in length. The results of these tests are also given in Table 1.

Twelve additional tests were done to determine the horizontal shear capacity along the contact interface. The “push-off” method [12,13] was used to determine this value. A schematic of the test rig is illustrated in Fig. 9. The precast member is braced and the in situ concrete is pushed with a ramping load until shearing along the interface occurs.

The dimensions of these beams (i.e., beams 1 through 12) are the same as the beams illustrated in Fig. 7, but the length was reduced to 750 mm. The prestressing information of Table 1 also correlates with each of the test beams (i.e., beams A1, 1 & 7; A2, 2 & 8, etc.). A set of six beams were tested when the in situ concrete strength reached 22.8 MPa and the other at 31.4 MPa (cube strengths). Two sets of tests were done to project the horizontal shear strength at different concrete strengths.

Since none of the test specimens contain shear reinforcement across the interface, the failure load was sudden and well defined. The shear capacity was calculated by dividing the failure load by the contact interface. The results of these tests are given in Table 2.

From Table 2, the following empirical equation was formulated by curve fitting to determine the horizontal shear strength (v_{nh}) at different concrete strengths:

Table 1
Failure load and prestress and concrete information of the test beams bent in flexure

Beam number	Concrete strength of precast members (MPa)	In situ concrete strength (MPa)	Number and height of strands above the soffit of the precast member	Strands diameter (mm)	Yield strength of strand (MPa)	Failure load (kN)
A1	42.7	31.0	3 @ 37 mm 2 @ 20 mm 2 @ 10 mm	4	1700	110
A2	42.7	31.0	3 @ 37 mm 2 @ 20 mm 2 @ 10 mm	4	1700	94
A3	42.7	16.6	1 @ 35 mm 2 @ 15 mm	4	1700	60
A4	42.7	16.6	4 @ 40 mm 4 @ 15 mm	4	1700	5
A5	42.7	20.8	1 @ 35 mm 2 @ 15 mm	4	1700	75
A6	42.7	20.8	1 @ 35 mm 2 @ 15 mm	4	1700	94

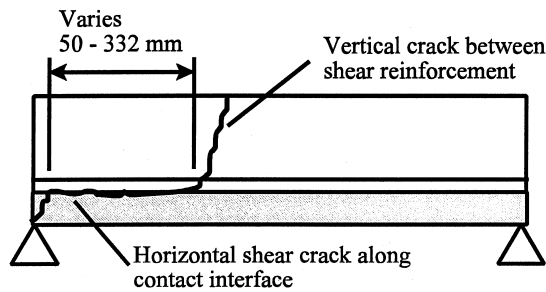


Fig. 8. Typical shear pattern in test beams bent in flexure.

$$v_{nh} = 0.025f_{cu} + 0.377. \quad (30)$$

Eq. (30) has not been reduced to an appropriate confidence interval nor have any safety or material factors been applied. For this reason, Eq. (30) should not be used for design purposes but is used in this study to verify the proposed equations.

Eqs. (21) and (29) are compared with the experimental data (Eq. (30)), the vertical shear equation of ACI 318 (Sec. 17.5.2), the alternative equation (Section

17.5.3 or Eq. (8) of this paper) and the equations endorsed by BS 8110 and SABS 0100. BS 8110 and SABS 0100 give a similar solution to the alternative equation of ACI 318, but the values are reduced by a material factor. This comparison is given in Table 3.

5. Conclusions

Close inspection of Table 3 implies that the proposed equations predict the horizontal shear better than ACI 318, BS 8110 and SABS 0100. In all six cases, the proposed equations predict a shear stress less than those predicted by the codes but greater than the actual failure load. In design, the horizontal shear should be taken as the largest value calculated by Eqs. (21) or (29).

It should be restated that the proposed equations are entirely consistent with Section 17.5.3 of ACI 318-95. The “segment”, referred to in this section, could be a differential segment or a segment equal to half the span [4].

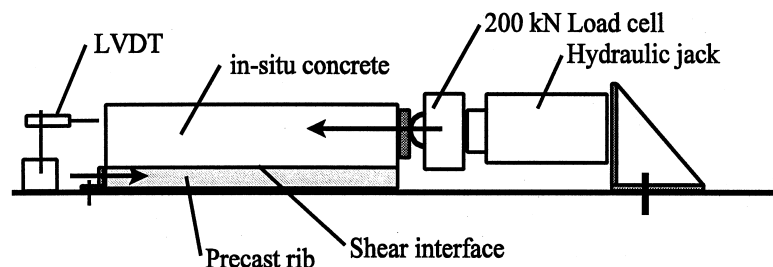


Fig. 9. Schematic of test rig.

Table 2

Horizontal shear capacity of test beams using the “push-off” method

Beam number	Horizontal shear strength (MPa)	Concrete strength (MPa)
1	1.05	In situ concrete strength: 22.8
2	0.69	
3	1.03	
4	1.25	Rib concrete strength: 41.7
5	0.79	
6	0.87	
7	1.24	In situ concrete strength: 31.4
8	1.27	
9	0.94	
10	1.15	Rib concrete strength: 41.7
11	1.11	
12	1.26	

Table 3

Comparison of the horizontal shear stress from experimental data, the proposed equations, ACI 318, BS 8110 and SABS 0100

Beam number	Eq. (21) uncracked section (MPa)	Eq. (29) cracked section (MPa)	ACI 318 Section 17.5.2 $V/b_v d$ (MPa)	ACI 318 Section 17.5.3 $4V_h/lb_v$ (MPa)	BS 8100 and SABS 0100 $4V_h/\gamma_m lb_v$ (MPa)	Experimental Eq. (30) (MPa)
A1	2.28	1.65	2.96	6.30	5.48	1.15
A2	1.95	1.41	2.53	6.30	5.48	1.15
A3	1.25	0.81	1.59	2.70	2.35	0.79
A4	0.95	0.67	1.23	7.20	6.26	0.79
A5	1.55	1.02	1.99	2.70	2.35	0.90
A6	1.94	1.28	2.50	2.70	2.35	0.90

In many international codes, the horizontal shear is based on the ultimate strength of the prestressing or reinforcement. The horizontal shear force will not exceed this value since the member will fail in flexure at this stage. The proposed equations differ in a sense that the calculation is not based on the flexural capacity, but calculates the horizontal shear at the point considered. This gives a more accurate representation of the horizontal shear. It is, however, based on a transformed section which is elastic theory. For this reason, it is not an exact representation but equations based on elastic theory are the simplest and most practical method for estimating the horizontal shear [11].

The experiments suggest that horizontal shear failure is not confined to a small region when shear reinforcement across the contact interface is omitted, but a failure mechanism is formed nearly reaching mid-span, in several cases. In addition, the failure was dramatic and seemingly instantaneous. This is in opposition to the commentary note of ACI 318-95 [1], which states that the slip along the interface is small and therefore only minimum redistribution occurs.

Acknowledgements

The author would like to acknowledge the Concrete Manufacturers' Association of South Africa for their financial support and assistance during this research.

References

- [1] ACI 318-95. Building code requirements for reinforced concrete. Detroit, Michigan: American Concrete Institute; 1995.
- [2] BS 8110-1:1997. Structural use of concrete. London: British Standards Institute; 1995.
- [3] SABS 0100-1:1992. The structural use of concrete. Pretoria: The Council of the South African Bureau of Standards; 1992.
- [4] Wang CK, Salmon CG. Reinforced concrete design. New York: Intext Publishers; 1973.
- [5] MacGregor JG. Reinforced concrete mechanics and design. 2nd ed. New Jersey: Prentice-Hall; 1988.
- [6] Mattock AH, Johal L, Chow HC. Shear transfer in reinforced concrete with moment or tension across the shear plane. PCI J 1975;20(4):76–93.
- [7] Misra A. Mechanistic model for contact between rough surfaces. ASCE J Eng Mech 1997;123(5):475–84.

- [8] Walraven J, Frenay J, Puijssers A. Influence of concrete strength and load history on the shear friction capacity of concrete members. *PCI J* 1987;33(1):166–8.
- [9] Ali MA, White RN. Enhanced contact model for shear friction and high strength concrete. *ACI Struct J* 1999;96(3):348–61.
- [10] Shaikh AF. Proposed revisions to the shear-friction provisions. *PCI J* 1978;23(2):12–21.
- [11] Loov R, Patnaik A. Horizontal shear strength of composite beams with a rough interface. *PCI J* 1994;39(1):48–67.
- [12] Lam D, Elliott KS, Nethercot DA. Push-off tests on shear studs with hollow-cored floor slabs. *Struct Eng* 1998;76(9):167–74.
- [13] Choi D-U, Jirsa JO, Fowler DW. Shear transfer across interface between new and existing concretes using large power-driven nails. *ACI Struct J* 1999;96(2):183–92.